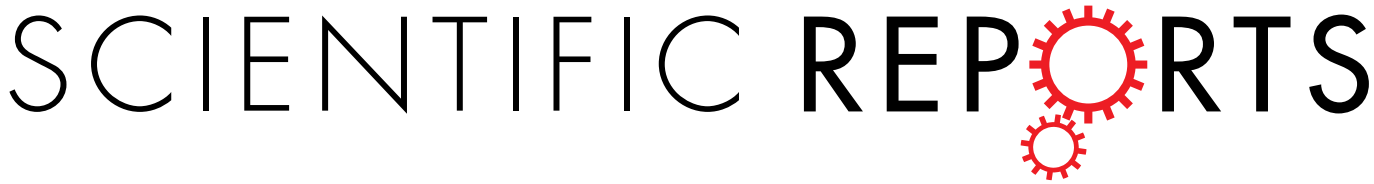

OPEN

Large-area functionalized CVD graphene for work function matched transparent electrodes

Received: 29 April 2015
Accepted: 28 September 2015
Published: 09 November 2015

Thomas H. Bointon[1], Gareth F. Jones[1], Adolfo De Sanctis[1], Ruth Hill-Pearce[2], Monica F. Craciun[1] & Saverio Russo[1]

The efficiency of flexible photovoltaic and organic light emitting devices is heavily dependent on the availability of flexible and transparent conductors with at least a similar workfunction to that of Indium Tin Oxide. Here we present the first study of the work function of large area (up to 9 cm^2) $FeCl_3$ intercalated graphene grown by chemical vapour deposition on Nickel, and demonstrate values as large as 5.1 eV. Upon intercalation, a charge density per graphene layer of $5 \cdot 10^{13} \pm 5 \cdot 10^{12}$ cm^{-2} is attained, making this material an attractive platform for the study of plasmonic excitations in the infrared wavelength spectrum of interest to the telecommunication industry. Finally, we demonstrate the potential of this material for flexible electronics in a transparent circuit on a polyethylene naphthalate substrate.

The development of flexible photovoltaic and light emitting devices depend on the availability and compatibility between flexible and transparent electrodes and photoactive materials. The most widely used transparent conductors nowadays -i.e. Indium-Tin-Oxide (ITO) and Fluorine doped Tin Oxide (FTO)- are brittle and their electrical properties degrade significantly under small applied strains[1–3]. Furthermore, the diffusion of Indium from ITO into photoactive layers of phovoltaic (PV) or organic light emitting diode (OLED) is also a well-known cause of device degradation[4]. The search for the best suitable transparent and flexible conductor is an open quest.

Meshes of metallic nano-wires are emerging as an attractive alternative, since they have high optical transmission (≈80% at 550 nm) and low sheet resistance (38Ω/□)[5] even when subjected to 16% strain[1]. However, scattering of light off nano-wires can introduce significant optical haze, limiting the range of applications for which these materials are suitable. Graphene is an emerging contender for enabling future flexible electronics. This single layer of sp2 hybridized carbon atoms has high optical transmission (97.6%)[6], does not suffer of haze and the conductance is unchanged even when subject to strains up to 6.2%[7]. Contrary to ITO, no carbon migration has been reported in PV and OLED that use graphene electrodes. However, the efficiency of these devices is still low owing to the high sheet resistance of graphene (>500Ω/□)[8] and poor matching of the work function of graphene and that of the photoactive layer.

The sheet resistance of functionalized CVD graphene reported to date still greatly exceeds that of ITO ≈8Ω/□ causing excessive dissipation in electrical devices[9–12]. The high sheet resistance sets an upper limit to the maximum transparent electrode area for example of use in OLED devices. Indeed, the potential drop across the area of a transparent electrode increases with its area, and this would result in gradients of light intensity over the surface of the OLED. Furthermore, since the work function of pristine graphene is comparable to that of ITO (4.6 eV for graphene and 4.8 eV for ITO[4]), pristine graphene electrodes require electron or hole blocking layers for efficient PVs to account for the large work function mismatch between the electrode and the photoactive layers. Changing the work function of the electrodes to match the highest occupied and lowest unoccupied molecular orbitals of the photoactive layer would minimise the barrier for charge tunnelling and reduce the energy loss of carrier thermalisation.

[1]Centre for Graphene Science, College of Engineering, Mathematics and Physical Sciences, University of Exeter, Exeter EX4 4QF, United Kingdom. [2]National Physical Laboratory, Teddington TW11 0LW, United Kingdom. Correspondence and requests for materials should be addressed to S.R. (email: S.Russo@exeter.ac.uk)

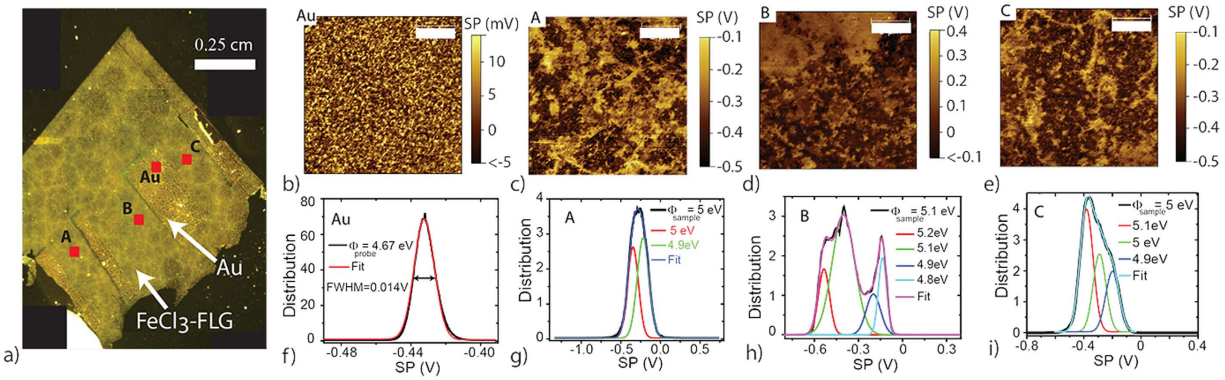

Figure 1. (**a**) Micrograph picture of an intercalated sample with Au contacts deposited on top. (**b–e**) SKPM maps of representative 20 μm^2 areas on Au and three other locations on $FeCl_3$-FLG as highlighted in the panel (**a**). (**f–i**) Graphs of the associated distributions to the SKPM maps shown in panels (**b–e**) reporting the calibrated Φ_{sample}. The tip was calibrated on an area of gold electrode shown in (**b**) with the corresponding distribution in (**f**). A Φ_{probe} of 4.67 eV was calculated assuming a Φ_{Au} of 5.1 eV.

Finding a transparent, flexible and highly conductive material that does not require charge blocking layers when embedded in PVs would enable the developement of conceptually new electronic applications.

Here we present the first experimental study of the work function (WF) of large area (up to 9 cm^2 on glass and up to 1 cm^2 on Si) $FeCl_3$-FLG obtained from Ni-grown graphene. We find values as high as 5.1 eV, that is 0.3 eV larger than the work function of ITO, making this material an ideal replacement for ITO in PV and OLED since it would not require the additional charge blocking layer typically used with ITO electrodes. With the aid of Raman spectroscopy, we estimate a charge density per graphene layer of $FeCl_3$-FLG up to $5 \cdot 10^{13} \pm 5 \cdot 10^{12}$ cm^{-2}, making this material an attractive platform for studying the physics of plasmons in the infrared region. Finally we demonstrate the potential of this material for flexible electronics in a transparent circuit on an insulating, transparent and flexible sheet of Polyethylene naphthalate (PEN) with a room-temperature resistivity of 20.52Ω/□ and high optical transmission of 77% in the visible wavelength range.

Results

Large-area multilayer graphene grown on nickel (Wafer of 100 mm Graphene Film on Nickel purchased from Graphene supermarket) was transferred to glass substrates by using PMMA as a support during the wet-etching of nickel in a $FeCl_3$ solution. The films were subsequently transferred to ultra pure water, to a concentrated HCl solution for 1 hour and rinsed in ultra pure water[13]. Finally, the stack of multilayer graphene/PMMA was transferred to glass substrates and, after 24 hours, the PMMA was removed with acetone. A study of the optical contrast shows that 35% of this material is a four-layer with an average domain area of 150μm^2, see Supplementary information. Two separate sets of multilayer graphene samples were intercalated with $FeCl_3$ for 8 and 24 hours following a previously demonstrated two-zone vapour transport method[14,15]. The resulting material is a heavily doped form of graphene highly stable to high levels of humidity (>95% relative humidity) and high temperature (up to 200°C in air and at least 650°C in vacuum)[16] which was previously shown to be a good replacement for gold electrodes in photodetectors devices[17].

Scanning Kelvin probe microscopy (SKPM) is used to determine the absolute work function (Φ) and its spatial distribution over the surface of intercalated graphene. SKPM maps the electrostatic forces between the surface of the sample and a conductive atomic force microscopy (AFM) probe which is oscillated above the sample surface. The electrostatic force between the cantilever and the sample is nullified by applying a backing dc bias to a conductive AFM probe. The applied bias which is equal and opposite to the electrostatic potential is termed the surface potential (SP) and is equivalent to the contact potential difference (V_{CPD}) measured in static Kelvin probe measurements. The accuracy with which the absolute work function of a material using Kelvin probe methods can be calculated depends on the accuracy with which the work function of the probe can be determined. For these measurements we employed an NT-MDT NTEGRA Aura system using frequency-modulated SKPM mode and conductive Bruker PFQNE tips in ambient conditions.

Gold electrodes were deposited onto the intercalated samples serving both as a grounding contact and a calibration standard for the measurements of Φ, see Fig. 1a–i. The Φ of the AFM probe was calibrated by comparison with that of the gold electrodes; ($\Phi_{probe} = \Phi_{Au} + V_{CPD}$) where Φ_{Au} is assumed to be 5.1 eV[18]. Gold is chosen as a standard in Kelvin probe measurements as it does not oxidise or readily undergo chemical reactions. A map of the spatial dependence of the SP of the gold film is shown in Fig. 1b. The corresponding SP distribution is found to be narrow demonstrating the homogeneity of Φ_{Au} with an average SP of −0.43 V and a full width at half maximum (FWHM) of 0.014 eV giving a Φ_{probe}

of 4.67 eV ± 8 meV, see Fig. 1f. Figure 1b–c,g–i show SKPM maps and SP distribution histograms for representative 20 μm^2 areas of the intercalated sample highlighted in the micrograph picture of Fig. 1a. Several distinct SPs are observed in the SKPM maps with distribution histograms showing overlapping peaks corresponding to a distribution of Φ_{sample}. The most commonly occurring Φ_{sample} were recorded at 5.1, 5 and, 4.9 eV with the majority of the surface area of the sample ≈60% showing a work function value as large as 5.1 eV (see Supporting information). The observed three dominant values of Φ_{sample} are to be expected in intercalated few-layer graphene and correspond to the following three distinct cases: (1) graphene sandwiched between $FeCl_3$, (2) graphene with $FeCl_3$ only on one side and (3) graphene with no direct contact to $FeCl_3$. While the SP was observed to vary on the nanoscale between 4.8–5.2 eV, the average Φ_{sample} value of 5 eV was uniform over the scale of the sample -that is 1 cm^2.

Raman spectroscopy is another valuable tool for the characterization of this material. Figure 2a shows a representative Raman spectra of a 1 cm^2 multilayer graphene on a Si/SiO_2 substrate intercalated for 36 h. We find that the G-band (1580–1630 cm^{-1}) is composed by four Lorentzian peaks labelled as G_0 (1580 cm^{-1}), G_1^* (1600 cm^{-1}), G_1 (1611 cm^{-1}) and G_2 (1622 cm^{-1}). Each G-peak corresponds to a different level of charge transfer[14,19,20]. Upon doping the 2D-band (≈2700 cm^{-1}) is upshifted and its shape becomes the convolution of a smaller number of Lorentzians as compared to the pristine multilayer graphene[21]. We find that four Lorentzians are needed to obtain a good fit to the 2D-band shown in Fig. 2a with maxima at 2637 cm^{-1} ($2D_0$), 2684 cm^{-1} ($2D_1^*$), 2700 cm^{-1} ($2D_1$) and 2721 cm^{-1} ($2D_2$).

The positions of G- and 2D- peaks are unique identifiers of the doping level in this intercalated compound. More specifically, G_0 and $2D_0$ are characteristic of un-doped (pristine) graphene layers. G_1 and $2D_1$ indicate that graphene is in direct contact to only one adjacent $FeCl_3$ layer (low doping), whereas G_2 and $2D_2$ appear when graphene is sandwiched between two $FeCl_3$ layers (high doping)[14]. G_1^* and $2D_1^*$ is attributed to graphene in direct contact to only one adjacent $FeCl_3$ layer but with a lower density of $FeCl_3$ molecules, thus giving lower charge transfer.

Discussion

To characterize the Fermi energy in $FeCl_3$-FLG from the Raman spectra we use the model developed by Lazzeri *et al.*[22] where doping of graphene stiffens the E_{2g} phonon mode of the Raman G-peak due to the non-adiabatic removal of the Kohn anomaly at Γ[23]. Within this model, a unique relation between the charge density n and the upshift of the G-peak position was obtained and this can efficiently be used to determine n with an accuracy better than 10% from the values of charge density obtained with complementary methods such as quantum oscillations of magneto-conductance, see Supplementary information. Estimates of n over a representative surface area of $10^4\,\mu m^2$ in our material show three different doping levels, see Fig. 2b. The presence of three distinct G-peaks in the Raman spectra allow us to extrapolate three corresponding charge concentrations: $n_0 = 0.3 \cdot 10^{13} \pm 1 \cdot 10^{12}\,cm^{-2}$, $n_1^* = 2.6 \cdot 10^{13} \pm 3 \cdot 10^{12}\,cm^{-2}$ and $n_1 = 4.6 \cdot 10^{13} \pm 5 \cdot 10^{12}\,cm^{-2}$, see Fig. 2c. In a $FeCl_3$-intercalated multilayer graphene system, such as Ni-grown CVD graphene, the total charge density can reach values as high as $10^{15}\,cm^{-2}$ for a sequence of 15 graphene layers.

Since the exploitation of collective charge oscillations in graphene (i.e. plasmons) for light manipulation strongly relies on doping, $FeCl_3$-intercalation of multilayer graphene provides an attractive platform for pioneering studies of surface plasmons at wavelengths of interest to the telecommunication industry. More specifically, the plasmon frequency in graphene scales as $\hbar\omega \propto (E_F/D)^{1/2}$ where E_F is the Fermi level and D is the size of the resonant plasmonic structure[24]. A Fermi energy of $E_F \approx 1\,eV$, corresponding to a total charge density of $\approx 7 \cdot 10^{14}\,cm^{-2}$, would give a plasmon resonance at a photon wavelegth of ~1.4μm[24]. Such a high charge density can be easily attained in $FeCl_3$-intercalated multilayer graphene.

The room temperature resistivity of the Ni-grown intercalated multilayer graphene was characterized by measuring the four-terminal resistance in devices with different aspect ratios of the conductive channel, that is device length -ranging from 0.15 cm to 0.7 cm- divided by the device width (1 cm), see Fig. 3a. A linear fit to these measurements gives a typical sample resistivity of 20.52 ± 0.48 Ω/□, which is ≈1000 times smaller than the resistivity of graphene at the neutrality point and more than 20 times smaller than the lowest values of resistivity reported in CVD-grown graphene to date. At the same time we find that the optical transmittance (T) of intercalated multi-layer graphene on a glass substrate in the visible wavelength range from 450 nm to 850 nm is larger than 74%, see Fig. 3b,c. In particular, at 550 nm T is higher than 77%, and this is comparable to the value for a 10μm film of ITO of 80%[12]. Upon increasing the wavelength to 850 nm the optical transmission increases monotonously to 87%.

The unique combination of (1) large work function, (2) low electrical resistivity and (3) high optical transmittance make this material an attractive system for flexible electronics and PV applications. To demonstrate further its potential, we have transferred the intercalated Ni-graphene to a standard flexible PEN substrate. This is readily done by spin coating PMMA onto $FeCl_3$-FLG and using a thermal release tape to mechanically peal the functionalized graphene off the glass substrate see Fig. 2c. Subsequently, the large area $FeCl_3$-FLG of 1 cm^2 was dry transferred to a PEN substrate, while the tape and PMMA are removed by a heat process and rinsing in acetone, respectively (see Fig. 3d). We then demonstrate the use of $FeCl_3$-FLG as a transparent conductor by closing the circuit of a battery lighting up an LED through this functionalized graphene, as shown in Fig. 3e. Note that owing to the high electrical conductivity of

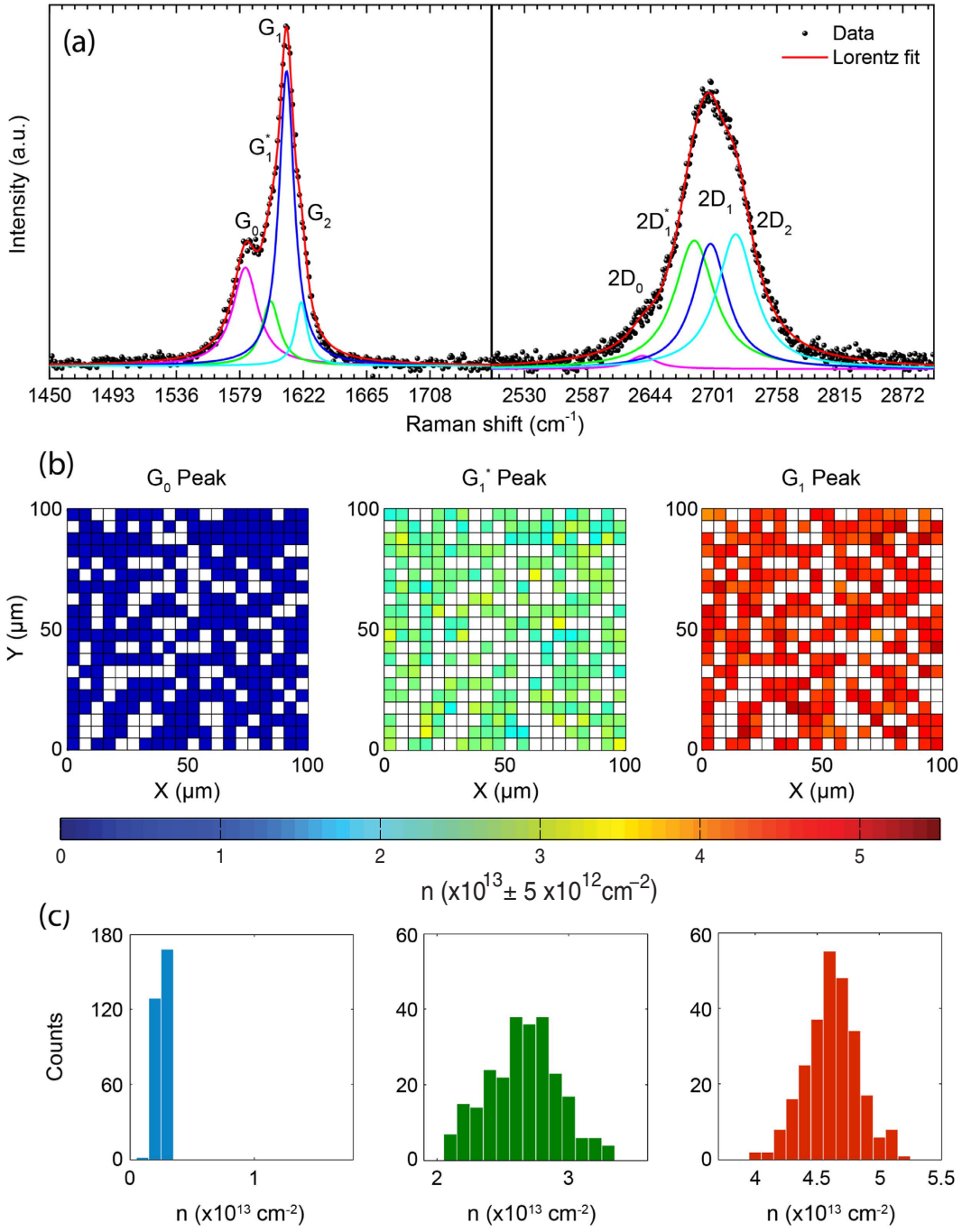

Figure 2. (**a**) Representative Raman spectrum (532 *nm* laser excitation) of large-area $FeCl_3$ intercalated few-layer graphene showing the G- (1580–1630 cm^{-1}) and 2D-band regions (≈2700 cm^{-1}) with the respective four Lorentzian peaks fit (G_0-$2D_0$, G_1^*-$2D_1^*$, G_1-$2D_1$ and G_2-$2D_2$). (**b**) Spatial distribution of the hole concentration for the first three intercalation stages, over an area of $100 \times 100\,\mu m^2$ mapped in steps of 5 μm. (**c**) Statistical study of n for each intercalation stage over the 400 points in (**b**).

this material, it is necessary to introduce a resistor in series to the circuit to limit the voltage drop across the LED to less than 2 V.

In conclusion we have presented the first systematic study of the work function of large area $FeCl_3$-FLG obtained from Ni-grown graphene (up to 9 cm^2 on glass and 1 cm^2 on Si and PEN), with values as large as 5.1 eV, which qualify this material as a replacement for ITO for example in PV and OLED. Upon intercalation, a charge density per graphene layer of $\approx 5 \cdot 10^{13}\,cm^{-2}$ is attained, making this material an attractive platform for the study of plasmons in the infrared region potentially of interest to the telecommunication industry. Finally, we demonstrate the potential of this material for flexible electronics in a transparent

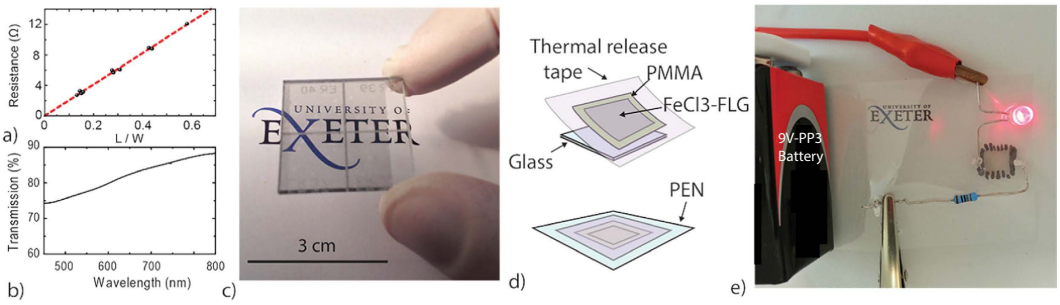

Figure 3. (**a**) Plot of the resistance as a function of the $FeCl_3$-FLG channel aspect ratio defined as length over width (L/W). (**b**) Plot of the optical transmittance in the visible wavelength range. The experimental error in transmittance is smaller than 0.1%. (**c**) Image of large-area FeCl3-FLG on a 9 cm^2 glass substrate made using a PMMA-assisted wet transfer technique. (**d**) Schematic representations of the dry transfer method used to transfer $FeCl_3$-FLG from a glass substrate to the target flexible and transparent PEN substrate. (**e**) Picture of an electric circuit which uses the $FeCl_3$-FLG on PEN as an electric line to light up a red LED.

circuit on a PEN substrate with a room temperature resistivity of 20.52Ω/□ and optical transmission of 77% in the visible wavelength range.

References

1. Yu, Z. *et al.* Highly Flexible Silver Nanowire Electrodes for Shape-Memory Polymer Light-Emitting Diodes. *Adv. Matt*. **23,** 664 (2011).
2. Cairns, D. R. *et al.* Strain-dependent electrical resistance of tin-doped indium oxide on polymer substrates, *App. Phys. Lett.* **76,** 1425 (2000).
3. Hecht, D. S., Hu, L. & Irvin, G. Emerging Transparent Electrodes Based on Thin Films of Carbon Nanotubes, Graphene, and Metallic Nanostructures. *Adv. Matt*. **23,** 1482 (2011).
4. Wu, J. *et al.* Organic Light-Emitting Diodes on Solution-Processed Graphene Transparent Electrodes. *ACS nano* **4,** 43 (2010).
5. Hu, L., Kim, H. S., Lee, J. Y., Peumans, P. & Cui, Y. Scalable Coating and Properties of Transparent, Flexible, Silver Nanowire Electrodes. *ACS Nano* **4,** 2955 (2010).
6. Lee, W. H. *et al.* Transparent Flexible Organic Transistors Based on Monolayer Graphene Electrodes on Plastic. *Adv. Matt*. **23,** 1752 (2011).
7. Verma, V. P., Das, S., Lahuru, I. & Choi, W. Large-area graphene on polymer film for flexible and transparent anode in field emission device. *Appl. Phys. Lett.* **96,** 3108 (2010).
8. Meyer, J. *et al.* Metal Oxide Induced Charge Transfer Doping and Band Alignment of Graphene Electrodes for Efficient Organic Light Emitting Diodes. *Sci. Rep*. **4,** 5380 (2014).
9. Song, Y., Fang, W., Hsu, A. L. & Kong, J. Iron (III) Chloride doping of CVD graphene. *Nanotechnology* **25,** 395701 (2014).
10. Sun, T. *et al.* Multilayered graphene used as anode of organic light emitting devices. *Appl. Phys. Lett.* **96,** 133301 (2010).
11. De Arco, L. G. *et al.* Continuous, Highly Flexible, and Transparent Graphene Films by Chemical Vapor Deposition for Organic Photovoltaics. *ACS nano* **4,** 2865 (2010).
12. Lee, J. Y., Connor, S. T., Cui, Y. & Peumans, P. Solution-Processed Metal Nanowire Mesh Transparent Electrodes. *Nano Lett.* **8,** 689 (2008).
13. Park, H. J., Meyer, J., Roth, S. & Skákalová, V. Growth and properties of few-layer graphene prepared by chemical vapor deposition. *Carbon* **48,** 1088 (2010).
14. Khrapach, I. *et al.* Novel Highly Conductive and Transparent Graphene-Based Conductors. *Adv. Matt*. **24** 2844 (2012).
15. Bointon, T. H. *et al.* Approaching Magnetic Ordering in Graphene Materials by FeCl3 Intercalation. *Nano Lett.* **14,** 1751 (2014).
16. Wehenkel, D. J. *et al.* Unforeseen high temperature and humidity stability of FeCl3 intercalated few layer graphene, *Sci. Rep*. **5,** 7609 (2015).
17. Withers, F., Bointon, T. H., Craciun, M. F. & Russo, S. All-Graphene Photodetectors. *ACS Nano* **7,** 5052 (2013).
18. Hansen, W. N. & Johnson, K. B. Work function measurements in gas ambient, *Surf. Sci*. **316,** 373 (1994).
19. Zhao, W., Tan, P. H., Liu, J. & Ferrari, A. C. Intercalation of Few-Layer Graphite Flakes with FeCl3: Raman Determination of Fermi Level, Layer by Layer Decoupling, and Stability. *J. Am. Chem. Soc.* **133,** 5941 (2011).
20. Zhan, D. *et al.* FeCl3-Based Few-Layer Graphene Intercalation Compounds: Single Linear Dispersion Electronic Band Structure and Strong Charge Transfer Doping. *Adv. Func. Matt*. **20,** 3504 (2010).
21. Das, A. *et al.* Monitoring dopants by Raman scattering in an electrochemically top-gated graphene transistor. *Nat. Nanotech*. **3,** 210 (2008).
22. Lazzeri, M. & Mauri, F. Nonadiabatic Kohn Anomaly in a Doped Graphene Monolayer. *Phys. Rev. Lett.* **97,** 266407 (2006).
23. Pisana, S. *et al.* Breakdown of the adiabatic Born-Oppenheimer approximation in graphene. *Nat Mater* **6,** 198 (2007).
24. Garca De Abajo, F. J. Graphene Plasmonics: Challenges and Opportunities. *ACS Photonics* **1,** 135 (2014).

Acknowledgements

S.R. and M.F.C acknowledge Financial support from EPSRC (Grant no. EP/J000396/1, EP/K017160/1, EP/K010050/1, EPG036101/1, EP/M001024/1, EPM002438/1), from Royal Society international Exchanges Scheme 2012/R3 and 2013/R2.

Author Contributions

M.F.C. and S.R. conceived and directed the experiment. T.H.B. and G.F.J. conducted the fabrication and electrical measurements. A.D. conducted the Raman spectroscopy measurements and G.F.J. conducted the

analysis of the charge density maps from the Raman spectra. R.H.P. conducted the KPM measurements and interpretation. All authors contributed to the writing of the paper and interpretation of the data.

Additional Information

Supplementary information accompanies this paper at http://www.nature.com/srep

Competing financial interests: The authors declare no competing financial interests.

How to cite this article: Bointon, T. H. *et al.* Large-area functionalized CVD graphene for work function matched transparent electrodes. *Sci. Rep.* **5**, 16464; doi: 10.1038/srep16464 (2015).